

## MIT Open Access Articles

*Ultrasound-guided percutaneous delivery of tissue-engineered endothelial cells to the adventitia of stented arteries controls the response to vascular injury in a porcine model*

The MIT Faculty has made this article openly available. **Please share** how this access benefits you. Your story matters.

**Citation:** Nugent, Helen M., Yin-Shan Ng, Desmond White, Adam Groothius, Glenn Kanner, and Elazer R. Edelman. "Ultrasound-Guided Percutaneous Delivery of Tissue-Engineered Endothelial Cells to the Adventitia of Stented Arteries Controls the Response to Vascular Injury in a Porcine Model." *Journal of Vascular Surgery* 56, no. 4 (October 2012): 1078–1088.

**As Published:** <http://dx.doi.org/10.1016/j.jvs.2012.03.002>

**Publisher:** Elsevier

**Persistent URL:** <http://hdl.handle.net/1721.1/102309>

**Version:** Author's final manuscript: final author's manuscript post peer review, without publisher's formatting or copy editing

**Terms of use:** Creative Commons Attribution-Noncommercial-NoDerivatives





Published in final edited form as:

*J Vasc Surg.* 2012 October ; 56(4): 1078–1088. doi:10.1016/j.jvs.2012.03.002.

## Ultrasound-guided percutaneous delivery of tissue-engineered endothelial cells to the adventitia of stented arteries controls the response to vascular injury in a porcine model

Helen M. Nugent, PhD<sup>a,b</sup>, Yin-Shan Ng, PhD<sup>a</sup>, Desmond White, BS<sup>a</sup>, Adam Groothuis, PhD<sup>b,c</sup>, Glenn Kanner, BS<sup>a</sup>, and Elazer R. Edelman, MD, PhD<sup>b,d</sup>

<sup>a</sup>Pervasis Therapeutics, Cambridge

<sup>b</sup>Harvard-M.I.T. Division of Health Sciences and Technology, Massachusetts Institute of Technology, Cambridge

<sup>c</sup>Concord BioMedical Sciences and Emerging Technologies, Lexington

<sup>d</sup>Cardiovascular Division, Brigham and Women's Hospital, Department of Medicine, Harvard Medical School, Boston

### Abstract

**Objective**—High restenosis rates are a limitation of peripheral vascular interventions. Previous studies have shown that surgical implantation of a tissue-engineered endothelium onto the adventitia surface of injured vessels regulates vascular repair. In the present study, we developed a particulate formulation of tissue-engineered endothelium and a method to deliver the formulation perivascular to injured blood vessels using a percutaneous, minimally invasive technique.

**Methods**—Stainless steel stents were implanted in 18 balloon-injured femoral arteries of nine domestic swine, followed by ultrasound-guided percutaneous perivascular injection of gelatin particles containing cultured allogeneic porcine aortic endothelial cells (PAE). Controls received injections of empty particles (matrix) or no perivascular injection (sham) after stent deployment. Animals were sacrificed after 90 days.

**Results**—Angiographic analysis revealed a significantly greater lumen diameter in the stented segments of arteries treated with PAE/matrix ( $4.72 \pm 0.12$  mm) compared with matrix ( $4.01 \pm 0.20$  mm) or sham ( $4.03 \pm 0.16$  mm) controls ( $P < .05$ ). Similarly, histologic analysis revealed that PAE/matrix-treated arteries had the greatest lumen area ( $20.4 \pm 0.7$  mm<sup>2</sup>;  $P < .05$ ) compared with

---

Copyright © 2012 by the Society for Vascular Surgery.

Reprint requests: Elazer R. Edelman, MD, PhD, Harvard-M.I.T. Division of Health Sciences and Technology, Massachusetts Institute of Technology, Cambridge, MA 02139 ere@mit.edu.

Author conflict of interest: Dr Nugent, Dr Ng, Mr White, and Mr Kanner are or were employees of and have shares in Pervasis Therapeutics. Elazer Edelman is on the board of directors and has shares in Pervasis Therapeutics.

The editors and reviewers of this article have no relevant financial relationships to disclose per the JVS policy that requires reviewers to decline review of any manuscript for which they may have a conflict of interest.

**Author Contributions:** Conception and design: HN, Y-SN, AG, GK, EE

Analysis and interpretation: HN, Y-SN, DW, AG, GK, EE

Data collection: Y-SN, DW, AG, GK

Writing the article: HN, EE

Critical revision of the article: HN, Y-SN, DW, EE

Final approval of the article: HN, Y-SN, DW, AG, GK, EE

Statistical analysis: HN, Y-SN, AG

Obtained funding: HN, EE

Overall responsibility: HN

controls ( $16.1 \pm 0.9 \text{ mm}^2$  and  $17.1 \pm 1.0 \text{ mm}^2$  for sham and matrix controls, respectively) and the smallest intimal area ( $3.3 \pm 0.4 \text{ mm}^2$ ;  $P < .05$ ) compared with controls ( $6.2 \pm 0.5 \text{ mm}^2$  and  $4.4 \pm 0.5 \text{ mm}^2$  for sham and matrix controls, respectively). Overall, PAE-treated arteries had a 33% to 50% decrease in percent occlusion ( $P < .05$ ) compared with controls. Histopathological analysis revealed fewer leukocytes present in the intima in the PAE/matrix group compared with control groups, suggesting that the biological effects were in part due to inhibition of the inflammatory phase of the vascular response to injury.

**Conclusions**—Minimally invasive, perivascular delivery of PAE/matrix to stented arteries was performed safely using ultrasound-guided percutaneous injections and significantly decreased stenosis. Application at the time of or subsequent to peripheral interventions may decrease clinical restenosis rates.

The most significant limitation of percutaneous revascularization of peripheral vessels due to atherosclerosis is the high rates of restenosis. Despite initial technical success, restenosis after angioplasty or stent implantation occurs in approximately 50% of the treated vessels, such as the superficial femoral artery (SFA), within 6 to 12 months.<sup>1-3</sup> Indeed, 1-year patency rates in the SFA range between 22% and 61% after bare metal stent implantation. While the use of drug-eluting stents in the coronary circulation has decreased restenosis rates, a benefit of stenting and drug elution in peripheral arteries has yet to be clearly demonstrated.<sup>4,5</sup> A study of sirolimus-coated stents in the SFA reported that the drug-eluting stents were not superior to bare metal stents.<sup>6</sup> Studies have demonstrated a benefit of paclitaxel-coated angioplasty balloons in the femoropopliteal artery<sup>7,8</sup> and of paclitaxel-coated stents in the SFA; however, long-term data in large, randomized clinical trials of peripheral arterial disease are lacking.

Vascular restenosis is a complex response to injury that occurs after all arterial interventions. The combined effects of local injury, thrombosis, inflammation and leukocyte infiltration, spasm, smooth muscle cell (SMC) proliferation, and vessel remodeling induce a hyperplastic response that encroaches on the blood vessel lumen.<sup>9,10</sup> In recent years, the adventitia has emerged as a key component of the vascular response to injury.<sup>11</sup> Endothelial cells (ECs), the major regulatory cells of the blood vessel, reside not only at the lumen interface but also within the adventitia and throughout the vessel as vasa vasorum. Experimental evidence suggests an association between vasa vasorum and neointimal formation after injury.<sup>12</sup> Therefore, it was postulated that supplementing the adventitial endothelium may provide control over the response to vascular injury. Indeed, open surgical placement of perivascular tissue-engineered ECs has been shown to inhibit intimal thickening, stenosis, and negative remodeling in experimental models of vascular injury.<sup>13-16</sup> While open field surgery is amenable to direct adventitial placement, the question arises as to whether tissue-engineered ECs could be applied by a minimally invasive technique and retain efficacy. Development of techniques to deliver viable, functional cells is essential to capitalize on the potential therapeutic impact and clinical utility of cell transplantation.<sup>17</sup> In the present study, we investigated the vascular response to stent-induced injury in porcine femoral arteries treated with gelatin particles containing allogeneic porcine aortic endothelial cells (PAE) injected adjacent to the affected vessel, using an ultrasound-guided visualization technique.

## Methods

### Endothelial cell culture on Gelfoam particles

PAE were isolated from the aorta of healthy pigs by collagenase digestion and cultured on gelatin particles (Gelfoam Powder; Pfizer, New York, NY) as previously described.<sup>18,19</sup> Growth on Gelfoam was evaluated by periodic evaluation of cell number after enzymatic

digestion.<sup>16</sup> Cell viability was assessed by trypan blue exclusion, and EC was allowed to reach a growth plateau prior to implantation. EC integrity was assessed by immunocytochemistry using a mouse antiporcine CD31 antibody (MCA1746G; AB-D Serotec, Raleigh, NC) to stain for platelet endothelial cell adhesion molecule (PECAM). Nonspecific binding sites were blocked with normal donkey serum. Alexa Fluor 488-conjugated donkey antimouse secondary antibody (1:300; Invitrogen, Grand Island, NY) was added, and cells were counterstained with 4',6-diamidino-2-phenylindole (DAPI). Control particles (matrix) were incubated for up to 2 weeks in medium prior to implantation.

### Biochemical and in vitro functional activity

Functional testing was performed on conditioned media from in vitro cohorts as previously described.<sup>13,19</sup> The production of heparan sulfate (HS), transforming growth factor- $\beta_1$  (TGF- $\beta_1$ ), nitric oxide (NO), and tissue inhibitor of metalloproteinase-2 (TIMP-2) were used as markers of EC function. HS levels in conditioned media were determined using a dimethyl methylene blue binding assay. TGF- $\beta_1$ , TIMP-2, and NO concentrations were determined by enzyme-linked immunosorbent assay (R&D Systems, Minneapolis, Minn). The ability of PAE on gelatin particles (PAE/matrix) to inhibit proliferation was determined using conditioned media in an SMC growth stimulation assay. Porcine aortic SMC were seeded in SMC growth medium (SmGM-2, Lonza BioScience [Walkersville, Md], contains 5% fetal bovine serum [FBS], fibroblast growth factor, and epidermal growth factor), allowed to attach for 24 hours, and growth arrested for 48 to 72 hours. Conditioned and control media was diluted 1:1 with  $2 \times$  SmGM-2 and added to the wells. Cell number was determined after 3 days by colorimetric analysis (CellTiter 96 Proliferation Assay; Promega, Madison, Wisc). Growth factor stimulation (GFS) was determined by dividing the absorbance (ABS) of conditioned or control media wells by the ABS for 5% FBS wells. The effect of conditioned media on SMC growth factor stimulation was then determined by the following equation:

$$\frac{(\text{SmGM} - 2 \text{ GFS}) - (\text{conditioned or control GFS})}{(\text{SmGM} - 2 \text{ GFS}) - 1} \times 100$$

The ability of PAE/matrix-conditioned media to suppress markers of inflammation and thrombosis was determined using real-time polymerase chain reaction (RT-PCR). Briefly, human aortic EC (HAE) were grown to confluence and serum-starved in 0.5% FBS for 24 hours. Cells were treated with endothelial basal medium supplemented with 0.5% FBS (control media) alone or supplemented with 1  $\mu\text{g}/\text{mL}$  of platelet factor-4 (PF-4; Peprotech, Rocky Hill, NJ) or with media conditioned by PAE/matrix supplemented with 1  $\mu\text{g}/\text{mL}$  of PF-4 for 3.5 hours. PF-4 is a proatherogenic platelet molecule that has been shown to increase E-selectin RNA as well as other inflammatory and thrombotic markers and was added to EC cultures to simulate an injured state.<sup>20</sup> RNA samples were harvested from each individual well using the RNeasy Mini spin column kit (Qiagen, Valencia, Calif) according to the manufacturer's protocol. The concentration of the representative RNA samples was determined using the Experion capillary electrophoresis apparatus with the Experion RNA StdSens analysis kit (Bio-Rad, Hercules, Calif). The resulting total RNA samples from each treatment group were used for RT-PCR analysis to determine the expression levels of various inflammatory and thrombotic genes (Table I). The “ $2^{-\Delta\Delta\text{Ct}}$ ” calculation for relative gene expression comparison method was used for PCR data analysis: the relative expression level of each gene ( $\text{Ct}_{\text{gene}}$ ) was first normalized to the house-keeping marker hypoxanthine ribosyltransferase (HPRT) to generate the  $\Delta\text{Ct}$  value ( $\text{Ct}_{\text{gene}} - \text{Ct}_{\text{HPRT}}$ ), which was then further normalized to the respective treatment control (control media with PF-4) to generate

the  $\delta\delta C_t$ . The  $2^{-\Delta\Delta C_t}$  value of each gene representing the relative expression level was calculated and plotted for data presentation.

### **In vivo biologic activity of transplanted endothelial cells**

The ability of the PAE/matrix to control vascular repair when injected adjacent to stented porcine femoral arteries was assessed. This study conformed to the guidelines specified in the National Institutes of Health “Guide for Care and Use of Laboratory Animals” and was approved by the Institutional Animal Care and Use Committee of Concord BioMedical Sciences and Emerging Technologies (Lexington, Mass). Male domestic pigs, 43.1 kg  $\pm$  0.9 kg at implant, were obtained from Animal Biotech, Inc (Danboro, Pa). Anesthesia was induced and animals monitored throughout the procedure as previously described.<sup>18</sup> To prevent or reduce the occurrence of thrombotic events, animals were treated on day 1 with aspirin (650 mg per os [PO]) and clopidogrel (300 mg, PO). The animals were then treated with aspirin (81 mg, PO) and clopidogrel (75 mg, PO) daily thereafter.

A total of nine pigs were implanted with stents in the right and left femoral arteries (total stented arteries, 18). This study was conducted in compliance with the Food and Drug Administration Good Laboratory Practice Regulations. Briefly, right carotid arterial access was obtained, and a 5.0-mm-diameter angioplasty balloon (Abbott Vascular, Redwood City, Calif) was advanced to the left and right femoral arteries under fluoroscopic guidance (GE 9800 C-arm fluoroscope [GE Healthcare, Wauwatoga, Wisc], resolution 15 frames per second). The right and left arteries were injured by 30-second balloon inflations at 10 atmospheres pressure (three inflations per side, in overlapping segments) to ensure adequate removal/injury of endogenous luminal endothelium. Biliary stents (5.5 mm  $\times$  18 mm, Herculink; Abbot Vascular) were introduced into the left and right femoral arteries. Angiography was performed, and the stents were expanded with the 5.0-mm-diameter angioplasty balloon at 10 to 12 atmospheres pressure. Heparin (50-200 U/kg intravenously) was administered to prolong activated clotting time (ACT) to a target range of  $\approx$  275 seconds during stent deployment. After final angiography to assess vessel patency, the femoral arteries were treated with minimally invasive injections of  $\approx$  70 mg/3.0 mL media of control matrix (n = 6 arteries, two arteries per animal), PAE/matrix (n = 6 arteries, two arteries per animal), or no perivascular injection (sham, n = 6 arteries, two arteries per animal) adjacent to the perivascular tissue of the stented artery. Contralateral arteries received the same treatment to allow for blood collection at 4, 8, and 12 weeks to assess differences in clinical pathology, hematological, serum chemistry, and coagulation parameters between treatment groups. Animals were euthanized at 90 days, and the femoral arteries plus stent were processed for histologic evaluation. For each artery, angiography was performed prior to injury, immediately after stent deployment, and on day 90. Quantitative angiography was performed on recorded images using Centricity Cardiology CA1000 Cardiac Review 1.0 (SpaII) QCA software in a blinded fashion (GE Healthcare). Measurements were also made of the reference unstented vessel and minimum lumen diameter (MLD) at 90 days.

To verify the location of the injected material, a separate non-Good Laboratory Practice study was performed in seven pigs. Stented and nonstented arteries were injected with either control particles stained with methyl blue or particles seeded with PAE. All pigs were sacrificed within 1 day, and tissue was isolated to determine the location of the injected material.

### **Ultrasound-guided percutaneous injections**

Control matrix or PAE/matrix was delivered to the perivascular site of stented femoral arteries percutaneously using a syringe and hypodermic needle. Delivery of the material was

visualized by ultrasound-guided needle placement techniques using echogenic needles (18G Chiba biopsy needle; Cook Medical, Bloomington, Ind). Aportable ultrasound system (model t-3000; Terason, Inc, Burlington, Mass) was used to visualize the targeted perivascular tissue, the needle position and movement, and to guide the placement of the material. Proximal and distal ends of the stent (visible under ultrasound) were used as landmarks to ensure that the injection site with respect to stent placement was similar among arteries. Injection target location was adjacent to the perivascular tissue.<sup>19</sup> Delivery to the sites was confirmed by continuous visualization of the injection site and blood flow during and postinjection by color-Doppler and spectral-Doppler ultrasound scan.

### Tissue processing

On the 90th postoperative day, animals were euthanized with intravenous potassium chloride (40 mEq). The femoral arteries were perfused at 100 mm Hg with Ringer's lactate solution, followed by 10% neutral formalin to fix the arteries in situ. The arteries were isolated and the vessel divided into five 10-mm-long segments: far proximal to the stent (1-3 mm upstream from the stent), proximal stent, middle of the stent, distal stent, and far distal to the stent (1-3 mm beyond the stent). The stented segments were methacrylate embedded and non-stented vessel segments were paraffin embedded. Slides with 5- $\mu$ m sections were obtained and stained with Mayer's hematoxylin and eosin and Verhoeff's van Gieson elastin stains. Leukocytes were identified after antigen retrieval at 80°C in 1 $\times$  Dako Target Retrieval solution for 2.5 hours and overnight incubation at 4°C with mouse antiporcine CD45, allotypic variant (clone: MAC323, AB-D Serotec; 1:10 dilution). The CSAII detection system (K1497; Dako Inc, Carpinteria, Calif) was used to detect primary antibody-tissue antigen binding. Porcine spleen was used as a positive control and antibody diluent solution was used as a negative control. PAE were identified as described above combined with avidin-biotin peroxidase complex or Alexa Fluor detection methods. All sections were counterstained with Mayer's hematoxylin solution (Sigma Chemical Co, St. Louis, Mo). Slides were read and interpreted by a board-certified veterinary pathologist blinded as to treatment groups. Histomorphologic findings were graded on a scale from 0 through 3, depending upon severity (0 = absent; 1 = present in tissue, but minimal feature; 2 = present in tissue, notable feature; 3 = present in tissue, overwhelming feature).<sup>21</sup>

Histomorphometric analysis was performed on all segments. The intimal thickness and area (I), lumen (L), media (M), and stent (S) areas were measured using a computerized digital planimetry system comprised of an Olympus DP-70 digital, BX-41 microscope and MicroSuite Biological (version 2.5) software. Measurements were made by a blinded observer of the proximal, middle, and distal segments for each vessel and averaged so that each vessel resulted in one data point. Comparisons were also made among groups for each of the proximal, middle, and distal planes.

### Statistical analysis

All data are presented as mean  $\pm$  standard error (SE). Statistical analysis comparing stented arteries of the different treatment groups used a one-way analysis of variance and a Tukey-Kramer multiple comparison test with JMP version 7.0.1 software (SAS Institute, Cary, NC). Differences were not considered significant unless the probability of the calculated statistic was less than 0.05.

## Results

### Biochemical and in vitro functional activity of PAE/Gelfoam

PAE/matrix were assayed for cell number, viability, TGF- $\beta$ <sub>1</sub>, HS, NO, and TIMP-2 production. PAE cultured on gelatin particles followed a growth pattern similar to that

observed for cells cultured on gelatin sponges (Fig 1).<sup>16</sup> The number of PAE recovered from the matrix increased exponentially from  $1.0 \times 10^4$  cells/mg on day 0 to  $6.8 \times 10^4$  cells/mg when they reached confluence (day 12–15). The viability of the recovered cells was approximately 90%. Thereafter, the cell number was fairly constant up to 8 days postconfluent (average of  $6.1 \times 10^4$  cells/mg on culture day 22). Significant levels of HS ( $0.632 \pm 0.09 \mu\text{g/mL/d}$ ), TIMP-2 ( $23.4 \pm 1.3 \text{ ng/mL/d}$ ), NO ( $1.1 \pm 1.1 \mu\text{mol/L/day}$ ), and TGF- $\beta_1$  ( $312 \pm 12.5 \text{ pg/mL/d}$ ) were detected in conditioned media collected from postconfluent in vitro cohorts. Moreover, PAE cultured on gelatin particles stained positive for the endothelial marker PECAM (Fig 1).

The inhibitory potential of PAE/matrix was further investigated in growth, thrombotic, and inflammatory assays. Conditioned medium inhibited growth factor stimulation of cultured SMC proliferation by  $36.3 \pm 1.6\%$  ( $P < .05$ ) and suppressed the PF-4 induction of various pro-thrombotic and proinflammatory gene expression in HAE. PAE/matrix-conditioned media significantly suppressed the PF-4 induction of vascular cell adhesion molecule-1 by  $69.7 \pm 2.7\%$  ( $P < .05$ ), intercellular adhesion molecule-1 by  $40.6 \pm 12.9\%$  ( $P < .05$ ), tissue factor (TF) by  $45.1 \pm 6.2\%$  ( $P < .05$ ), E-selection by  $82.3 \pm 2.9\%$  ( $P < .05$ ), and interleukin-8 by  $71.6 \pm 4.9\%$  ( $P < .05$ ; Fig 1).

### In vivo efficacy of perivascular endothelial cells

The pigs used in this study were randomly selected to receive one of the following treatments by ultrasoundguided percutaneous injection of gelatin particles into the perivascular tissue of stented femoral arteries: PAE/matrix, control matrix, or nothing (sham). All injections occurred without incident (Fig 2). Acute dissection to the femoral arteries in seven pigs confirmed location of the material and PAE directly adjacent to the adventitia of the artery and that a single injection of 70 mg/3 mL covered the length of the stented segment (Fig 2). The remaining animals were euthanized at 90 days. All incisions healed well, and all animals gained weight throughout the postoperative period. Mean hematologic and clinical chemistry values from all groups were similar and within expected ranges. All of the femoral arteries were patent at the 90-day time point. Angiographic analysis performed at 90 days postinjury revealed less stenosis and significantly greater MLD in the stented segments of arteries treated with PAE/matrix (Fig 3; Table II;  $P < .05$ ). There was no difference in MLD of sham arteries compared with arteries that received control particles. Morphometric analysis revealed similar results (Fig 3; Table III). Treatment with PAE/matrix reduced the intimal area from  $6.20 \pm 0.50 \text{ mm}^2$  and  $4.4 \pm 0.50 \text{ mm}^2$  for sham and matrix controls, respectively, to  $3.3 \pm 0.40 \text{ mm}^2$  ( $P < .05$ ). PAE/matrix also significantly increased the lumen area from  $16.1 \pm 0.90 \text{ mm}^2$  and  $17.1 \pm 1.0 \text{ mm}^2$  for sham and matrix controls, respectively, to  $20.4 \pm 0.70 \text{ mm}^2$  ( $P < .05$ ) and decreased the % occlusion compared to sham and matrix controls by 50% and 33%, respectively ( $P < .05$ ). The average intimal area of arteries treated with control matrix was less than the sham controls ( $P < .05$ ; Table III). However, when individual planes (proximal, mid, distal; Fig 4) were analyzed, only the PAE/matrix group had statistically significant less intimal area than the sham control group. There was no difference in stent diameter observed among groups at 90 days. There were no adverse edge effects observed in the far-proximal or fardistal sections of any of the animals.

Histopathological analysis (Table IV) revealed no adverse effects from perivascular injection of gelatin particles on the perivascular tissue or tissue healing response within the adjacent stented femoral arteries. Inflammation at the delivery site, intimal fibrin, adventitial fibrosis, and SMC necrosis were all minimal and comparable between groups. Injury score and adventitial vascularization were also assessed with no significant differences among groups. Endothelialization was generally complete and comparable among treatment groups (Fig 5). Neointimal hypocellularity, which generally increases in areas of mural injury with

increased neointimal production, was significantly greater in the two control groups compared with the PAE/matrix group (Fig 5). Fewer leukocytes (identified by CD45 staining; Fig 5) were present in the intima in the PAE/matrix group compared with the matrix (average difference of one severity point) and sham (average difference of two severity points) control groups. No positive staining for CD45 was observed in the media of any animals. Minimal CD45 staining was present in the adventitia with no differences observed between groups.

## Discussion

Despite the improvements in endovascular techniques in the last 20 years, restenosis is still a significant limitation of most arterial interventions performed in the peripheral circulation.<sup>8</sup> In particular, interventional treatments in the SFA have long suffered from excessively high restenosis rates regardless of treatment with balloon angioplasty and stenting.<sup>5,22</sup> Several studies have also reported stent fractures when used in the SFA that have been associated with angiographic (>50%) stenosis. Currently, no large, randomized trials have shown significant clinical benefit with the use of drug-eluting stents<sup>6</sup> or other agents such as glycoprotein IIb/IIIa platelet receptor-blocking agents<sup>23</sup> for restenosis associated with peripheral arterial interventions.

The endothelial technology presented here represents a novel approach to addressing the complications associated with peripheral interventions. The use of ECs to modify intravascular injury has been under active investigation for some time, primarily in the form of methods to endothelialize stents and/or the damaged native vessel.<sup>24,25</sup> However, the ability of ECs to regulate neointimal formation may not be limited to a luminal location, and studies have suggested that the adventitia and vasa vasorum influence the vessel response to injury.<sup>11,12</sup> Perivascular placement also presents a desirable location for logistical reasons – the cells and their secreted factors are not diluted or rapidly cleared by convective flow, nor do they impede flow. Indeed, implantation of perivascular, allogeneic tissue-engineered ECs has been shown to regulate the response to vascular injury and decrease stenoses<sup>13-16,26</sup> and has been investigated in the clinical setting of arteriovenous access for hemodialysis.<sup>27</sup> However, all of these studies utilized a porous, three-dimensional sponge as the support matrix for implantation of quiescent and therapeutic ECs. The application of this technology was therefore limited to those that require an open surgical procedure. An aim of the present study was to determine if this technology could be adapted to an injectable formulation and delivered utilizing a minimally invasive procedure, and if such a delivery would produce efficacy in vivo. The necessity of culturing ECs on matrices prior to implantation rather than direct injection of cell suspensions has been demonstrated previously.<sup>28-31</sup> ECs are anchorage-dependant and require attachment to a substrate for optimal viability and function.<sup>16,28,32</sup> Indeed, recent literature has highlighted the importance of developing transplantable scaffolds that optimize cell attachment, viability, and function to the widespread use and success of cell transplantation to treat or prevent organ and tissue failure.<sup>17</sup> It has also been shown that matrix-adhered ECs have significantly reduced expression of constitutive and cytokine-upregulated costimulatory and adhesion molecules compared with free ECs, and in particular, a marked abrogation of MHC II-regulated immune reactivity, resulting in muted host immune reaction to both allogeneic or xenogeneic matrix-adhered ECs.<sup>28</sup> We therefore developed a matrix-embedded EC formulation that was amenable to minimally invasive injection while maintaining a regulatory phenotype that maximally controlled inflammation, intimal thickening, and mural remodeling.

PAE were grown on gelatin particles and secreted similar levels of HS, TGF- $\beta$ <sub>1</sub>, FGF-2, NO, and TIMP-2 to that from cells grown on the sponges, suggesting that both types of matrices



supported the quiescent and therapeutic endothelial phenotype.<sup>33</sup> This was confirmed in vivo by the ability of PAE/matrix, injected percutaneously under ultrasound guidance, to inhibit intimal formation and stenosis in a porcine femoral stent model. A stent model was used to assess the ability of the PAE/matrix to control the response to a chronic vascular injury and to precisely locate the area of injury at a late time point. Because the PAE/matrix, as well as the gelatin matrix alone, degrades in vivo within 6 to 8 weeks, a 90-day time point was selected for this study to assess the durability of therapeutic effects.<sup>14,15</sup> Stented arteries in the PAE/matrix group had significantly greater MLD by angiography and significantly greater lumen area and less intimal formation compared with sham controls by histology at 90 days. It is interesting to note that upon initial evaluation of histologic samples, the injection of matrix alone, while not as great a difference as injection of matrix containing PAE, appeared to have some beneficial effects on intimal area compared with the sham control. However, upon further detailed analysis of histologic planes (Fig 4), there was no significant therapeutic effect of the matrix group. This was also the case for the angiographic analysis; control sham and matrix groups had almost identical MLD, while the PAE/matrix groups have a significantly larger MLD. Furthermore, it also appears that only the PAE/matrix group truly inhibited leukocyte infiltration into the intima. It is therefore more likely that the therapeutic benefits are due to the presence of the matrix-embedded cells and not the matrix alone.

Adverse events that have been associated with drug-eluting stents include inflammation, fibrin deposition, medial necrosis, intra-arterial hemorrhage, and incomplete healing or endothelialization at the stent struts.<sup>34</sup> All of these phenomena were evaluated in the present study. All stented vessels were completely endothelialized by the 90-day time point. There was no increase in inflammation, fibrin deposition, or medial necrosis due to the presence of perivascular PAE/matrix. Indeed, analysis of CD45-stained tissue sections from PAE/matrix animals revealed no leukocytes present in the intima of the arterial segments, compared with a moderate degree of CD45<sup>+</sup> cells in the control groups. This observation suggests that perivascular ECs, or factors released by the cells, may provide control over intimal formation by influencing the inflammatory phase of the vascular response to stent-induced injury.<sup>9,10,35</sup> This is similar to the proposed mechanism of mesenchymal stem cell (MSC) transplantation, where MSCs have been shown to modulate T-cell-mediated immunologic responses and inhibit dendritic cell maturation through paracrine interactions with MSC-soluble factors.<sup>29,36</sup> The in vivo data are further supported by the in vitro results. Conditioned media collected from PAE grown on gelatin particles suppressed PF-4 induction of prothrombotic and proinflammatory genes in cultured HAE and inhibited growth factor-stimulated SMC proliferation.

In addition, placement of the PAE/matrix in the adventitia and not associated with a stent has the advantage of allowing for application in clinical settings where stent placement may not be feasible, such as arteries located below the knee. A limitation of the present study was that the animals were healthy, and therefore the impact of angioplasty and stenting of an existing lesion was not assessed; however, the results suggest that percutaneous delivery of tissue-engineered EC to the adventitia promotes vascular repair after stent-induced injury. Injections of tissue-engineered ECs coincident with balloon angioplasty or stenting of peripheral arteries may improve the longterm success rates of these procedures. A clinical study assessing the safety and feasibility of ultrasound-guided percutaneous injections of tissue-engineered endothelium (derived from allogeneic human aortic endothelial cells) in patients undergoing stent placement in the SFA is currently ongoing.

## Acknowledgments

The authors thank Gee Wong, Philip Seifert, and James Stanley of Concord BioMedical Sciences and Emerging Technologies for their expert technical assistance in the pathologic evaluation of tissue sections.

Supported by Pervasis Therapeutics and by grants from the USA National Institutes of Health (R01 GM 49039) (E.E.).

## References

1. Minar E, Pokrajac B, Maca T, Ahmadi R, Fellner C, Mittlböck M, et al. Endovascular brachytherapy for prophylaxis of restenosis after femoropopliteal angioplasty: results of a prospective randomized study. *Circulation*. 2000; 102:2694–9. [PubMed: 11094034]
2. Grimm J, Müller-Hülsbeck S, Jahnke T, Hilbert C, Brossmann J, Heller M. Randomized study to compare PTA alone versus PTA with Palmaz stent placement for femoropopliteal lesions. *J Vasc Interv Radiol*. 2001; 12:935–42. [PubMed: 11487673]
3. Cejna M, Thurnher S, Illiasch H, Horvath W, Waldenberger P, Hornik K, et al. PTA versus Palmaz stent placement in femoropopliteal artery obstructions: A multicenter prospective randomized study. *J Vasc Interv Radiol*. 2001; 12:23–31. [PubMed: 11200349]
4. Tepe G. Drug-eluting stents for infrainguinal occlusive disease: progress and challenges. *Semin Vasc Surg*. 2006; 19:102–8. [PubMed: 16782516]
5. Machan L. Drug eluting stents in the infrainguinal circulation. *Tech Vasc Interv Radiol*. 2004; 7:28–32. [PubMed: 15071778]
6. Duda SH, Bosiers M, Lammer J, Scheinert D, Zeller T, Oliva V, et al. Drug-eluting and bare nitinol stents for the treatment of atherosclerotic lesions in the superficial femoral artery: long-term results from the SIROCCO trial. *J Endovasc Ther*. 2006; 13:701–10. [PubMed: 17154704]
7. Tepe G, Zeller T, Albrecht T, Heller S, Schwarzwälder U, Beregi JP, et al. Local delivery of paclitaxel to inhibit restenosis during angioplasty of the leg. *N Engl J Med*. 2008; 358:689–99. [PubMed: 18272892]
8. Werk M, Langner S, Reinkensmeier B, Boettcher HF, Tepe G, Dietz U, et al. Inhibition of restenosis in femoropopliteal arteries: paclitaxel-coated versus uncoated balloon: femoral paclitaxel randomized pilot trial. *Circulation*. 2008; 118:1358–65. [PubMed: 18779447]
9. Phillips-Hughes J, Kandarpa K. Restenosis: pathophysiology and preventive strategies. *J Vasc Interv Radiol*. 1996; 7:321–33. [PubMed: 8761807]
10. Virmani R, Farb A. Pathology of in-stent restenosis. *Curr Opin Lipidol*. 1999; 10:499–506. [PubMed: 10680043]
11. Rey FE, Pagano PJ. The reactive adventitia: fibroblast oxidase in vascular function. *Arterioscler Thromb Vasc Biol*. 2002; 22:1962–71. [PubMed: 12482820]
12. Kwon HM, Sangiorgi G, Ritman EL, Lerman A, McKenna C, Virmani R, et al. Adventitial vasa vasorum in balloon-injured coronary arteries: visualization and quantitation by a microscopic three-dimensional computed tomography technique. *J Am Coll Cardiol*. 1998; 32:2072–9. [PubMed: 9857895]
13. Nugent HM, Sjin RT, White D, Milton LG, Manson RJ, Lawson JH, et al. Adventitial endothelial implants reduce matrix metalloproteinase-2 expression and increase luminal diameter in porcine arteriovenous grafts. *J Vasc Surg*. 2007; 46:548–56. [PubMed: 17826244]
14. Nugent HM, Edelman ER. Endothelial implants provide long-term control of vascular repair in a porcine model of arterial injury. *J Surg Res*. 2001; 99:228–34. [PubMed: 11469891]
15. Nugent HM, Groothuis A, Seifert P, Guerrero JL, Nedelman M, Mohanakumar T, et al. Perivascular endothelial implants inhibit intimal hyperplasia in a model of arteriovenous fistulae: a safety and efficacy study in the pig. *J Vasc Res*. 2002; 39:524–33. [PubMed: 12566978]
16. Nugent HM, Rogers C, Edelman ER. Endothelial implants inhibit intimal hyperplasia after porcine angioplasty. *Circ Res*. 1999; 84:384–91. [PubMed: 10066672]
17. Soto-Gutierrez A, Yagi H, Uygun BE, Navarro-Alvarez N, Uygun K, Kobayashi N, et al. Cell delivery: from cell transplantation to organ engineering. *Cell Transplant*. 2010; 19:655–65. [PubMed: 20525441]

18. Dinbergs ID, Brown L, Edelman ER. Cellular response to transforming growth factor-beta1 and basic fibroblast growth factor depends on release kinetics and extracellular matrix interactions. *J Biol Chem.* 1996; 271:29822–9. [PubMed: 8939921]
19. Nugent HM, Ng YS, White D, Groothuis A, Kanner G, Edelman ER. Delivery site of perivascular endothelial cell matrices determines control of stenosis in a porcine femoral stent model. *J Vasc Interv Radiol.* 2009; 20:1617–24. [PubMed: 19854069]
20. Yu G, Rux AH, Ma P, Bdeir K, Sachais BS. Endothelial expression of E-selectin is induced by the platelet-specific chemokine platelet factor 4 through LRP in an NF-kappaB-dependent manner. *Blood.* 2005; 105:3545–51. [PubMed: 15591119]
21. Schwartz RS, Edelman ER, Carter A, Chronos NA, Rogers C, Robinson KA, et al. Preclinical evaluation of drug-eluting stents for peripheral applications: recommendations from an expert consensus group. *Circulation.* 2004; 110:2498–505. [PubMed: 15492330]
22. Schlager O, Dick P, Sabeti S, Amighi J, Mlekusch W, Minar E, et al. Long-segment SFA stenting—the dark sides: in-stent restenosis, clinical deterioration, and stent fractures. *J Endovasc Ther.* 2005; 12:676–84. [PubMed: 16363897]
23. Ansel GM, Silver MJ, Botti CF Jr, Rocha-Singh K, Bates MC, Rosen-field K, et al. Functional and clinical outcomes of nitinol stenting with and without abciximab for complex superficial femoral artery disease: a randomized trial. *Catheter Cardiovasc Interv.* 2006; 67:288–97. [PubMed: 16408299]
24. van Beusekom HM, ErtasG, Sorop O, Serruys PW, van der Giessen WJ. The Genous endothelial progenitor cell capture stent accelerates stent re-endothelialization but does not affect intimal hyperplasia in porcine coronary arteries. *Catheter Cardiovasc Interv.* 2012; 79:231–42. [PubMed: 21834062]
25. Lichtenen A, Tudorache I, Cebotari S, Suprunov M, Tudorache G, Goerler H, et al. Preclinical testing of tissue-engineered heart valves re-endothelialized under simulated physiological conditions. *Circulation.* 2006; 114(1 Suppl):I559–565. [PubMed: 16820637]
26. Nugent MA, Nugent HM, Iozzo RV, Sanchack K, Edelman ER. Perlecan is required to inhibit thrombosis after deep vascular injury and contributes to endothelial cell-mediated inhibition of intimal hyperplasia. *Proc Natl Acad Sci U S A.* 2000; 97:6722–7. [PubMed: 10841569]
27. Conte MS, Nugent HM, Gaccione P, Guleria I, Roy-Chaudhury P, Lawson JH. Multicenter phase I/II trial of the safety of allogeneic endothelial cell implants after the creation of arteriovenous access for hemodialysis use: the V-HEALTH study. *J Vasc Surg.* 2009; 50:1359–68 e1351. [PubMed: 19958986]
28. Methe H, Nugent HM, Groothuis A, Seifert P, Sayegh MH, Edelman ER. Matrix embedding alters the immune response against endothelial cells in vitro and in vivo. *Circulation.* 2005; 112(9 Suppl):I89–95. [PubMed: 16159871]
29. Methe H, Hess S, Edelman ER. Endothelial cell-matrix interactions determine maturation of dendritic cells. *Eur J Immunol.* 2007; 37:1773–84. [PubMed: 17559179]
30. Methe H, Edelman ER. Cell-matrix contact prevents recognition and damage of endothelial cells in states of heightened immunity. *Circulation.* 2006; 114(1 Suppl):I233–238. [PubMed: 16820578]
31. Methe H, Groothuis A, Sayegh MH, Edelman ER. Matrix adherence of endothelial cells attenuates immune reactivity: induction of hyporesponsiveness in allo- and xenogeneic models. *FASEB J.* 2007; 21:1515–26. [PubMed: 17264166]
32. Methe H, Hess S, Edelman ER. Endothelial immunogenicity—a matter of matrix microarchitecture. *Thromb Haemost.* 2007; 98:278–82. [PubMed: 17721607]
33. Bobik A, Campbell JH. Vascular derived growth factors: cell biology, pathophysiology, and pharmacology. *Pharmacol Rev.* 1993; 45:1–42. [PubMed: 8475168]
34. Farb A, Heller PF, Shroff S, Cheng L, Kolodgie FD, Carter AJ, et al. Pathological analysis of local delivery of paclitaxel via a polymer-coated stent. *Circulation.* 2001; 104:473–9. [PubMed: 11468212]
35. Rogers C, Welt FG, Karnovsky MJ, Edelman ER. Monocyte recruitment and neointimal hyperplasia in rabbits. Coupled inhibitory effects of heparin. *Arterioscler Thromb Vasc Biol.* 1996; 16:1312–8. [PubMed: 8857930]

36. Yagi H, Soto-Gutierrez A, Parekkadan B, Kitagawa Y, Tompkins RG, Kobayashi N, et al. Mesenchymal stem cells: mechanisms of immunomodulation and homing. *Cell Transplant*. 2010; 19:667–79. [PubMed: 20525442]

### Clinical Relevance

Endovascular interventions performed in the peripheral circulation are limited by restenosis. Thrombosis, inflammation, smooth muscle cell proliferation, and negative remodeling result in significant obstruction to the blood vessel lumen. While some trials have shown the beneficial effects of drug-eluting stents, data from large, randomized controlled clinical trials of peripheral arterial disease are lacking. In a large animal model of peripheral arterial stenting, we demonstrated that perivascular, ultrasound-guided injections of matrix-embedded endothelial cells significantly increased lumen diameter and decreased stenosis at 90 days. Development of techniques to deliver viable, functional cells is essential to realize the potential therapeutic impact of cell transplantation and expands the opportunity for the clinical application of cell-based therapy subsequent to endovascular interventions for peripheral arterial disease.

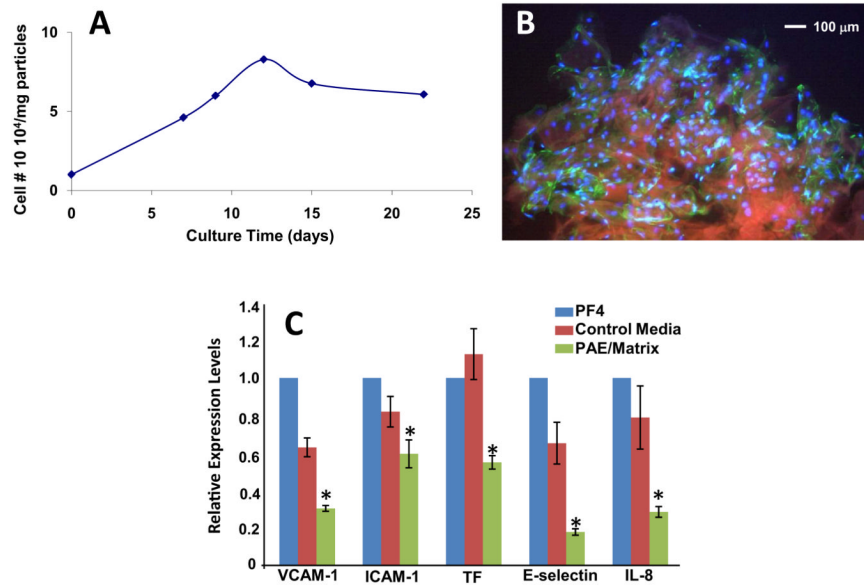


**Fig 1.** Characterization of porcine aortic endothelial cells (*PAE*) on gelatin particles. **A**, *PAE* cultured on particles followed a growth pattern similar to cells grown on sponges or standard tissue culture plastic. **B**, The preservation of endothelial cell integrity was determined by platelet endothelial cell adhesion molecule (PECAM) staining. *Green* cells indicate positive PECAM staining; *blue* indicates nuclei. **C**, Suppression of platelet factor-4 (*PF-4*) induced inflammatory and thrombotic gene expression on human aortic endothelial cells (HAE) by *PAE*/matrix-conditioned media. *ICAM-1*, Intercellular adhesion molecule-1; *IL-8*, interleukin-8; *TF*, tissue factor; *VCAM-1*, vascular cell adhesion molecule-1. \* $P < .05$  compared with *PF-4* and control media.

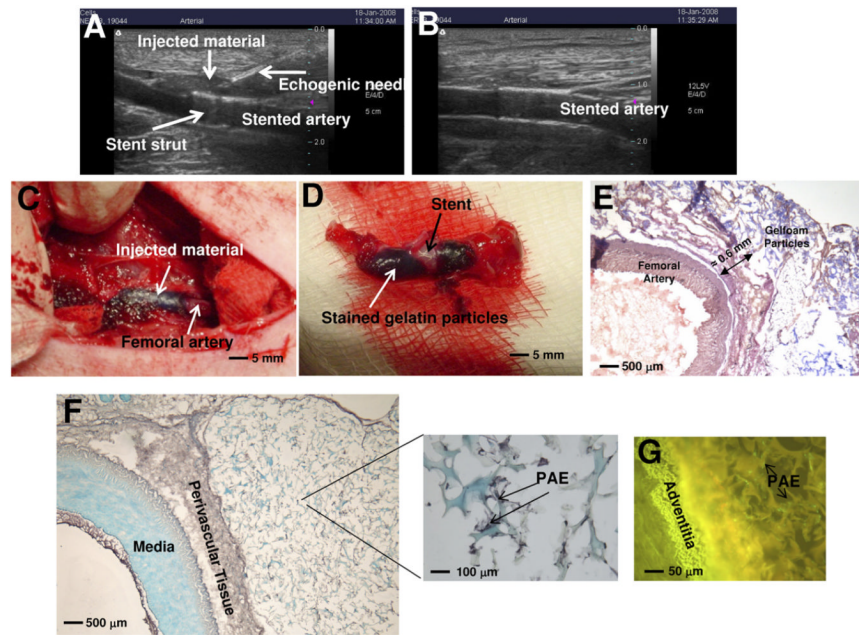


**Fig 2.** Images depict ultrasound-guided percutaneous delivery of porcine aortic endothelial cells (*PAE*)/matrix adjacent to perivascular tissue of femoral arteries (**A**) at the time of injection and (**B**) postinjection. **C** and **D**, Delivery site adjacent to the femoral artery was confirmed after femoral cutdown. Stent struts are visible within the artery, which is encapsulated with injected methyl blue-stained gelatin particles. **E**, Histologic section of unstented femoral artery stained with Mayer's hematoxylin solution confirms delivery of particles adjacent to perivascular tissue. **F** and **G**, Sections of unstented femoral arteries stained with CD31 identifies retention of *PAE* within the particles after percutaneous injection adjacent to the perivascular tissue.

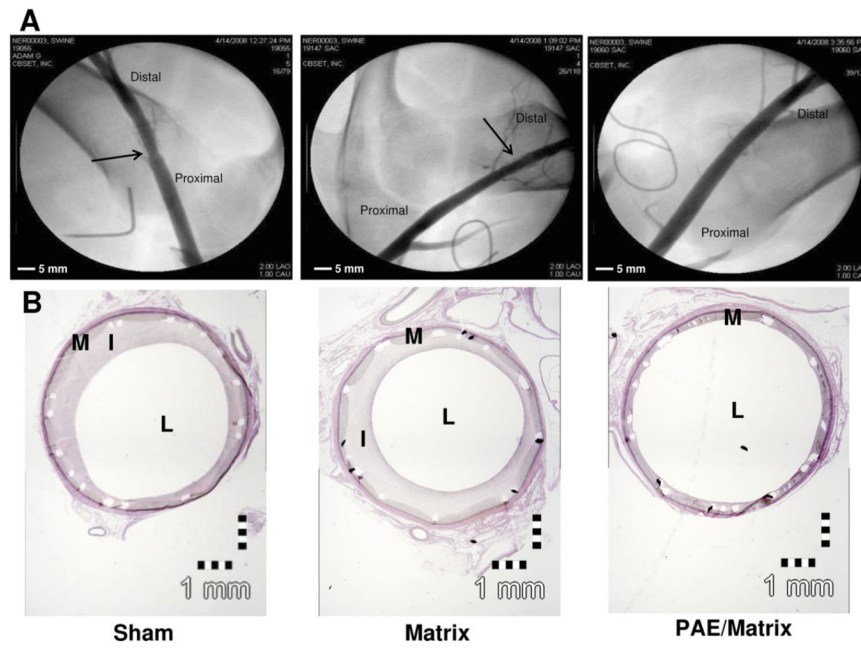


**Fig 3.** Representative day-90 angiograms (**A**) and photomicrographs of Verhoeff's elastin-stained arterial cross-sections (**B**). Comparison of the angiograms shows an increase in stenosis in the stented region of control arteries (*left and middle panels, black arrows*) compared with arteries treated with porcine aortic endothelial cells (*PAE*)/matrix (*right panel*). Histologic sections show significantly greater intimal area in control sham (*left panel*) and matrix (*middle panel*) arteries compared with arteries treated with perivascular PAE/matrix. *I*, Intima; *L*, lumen; *M*, media.



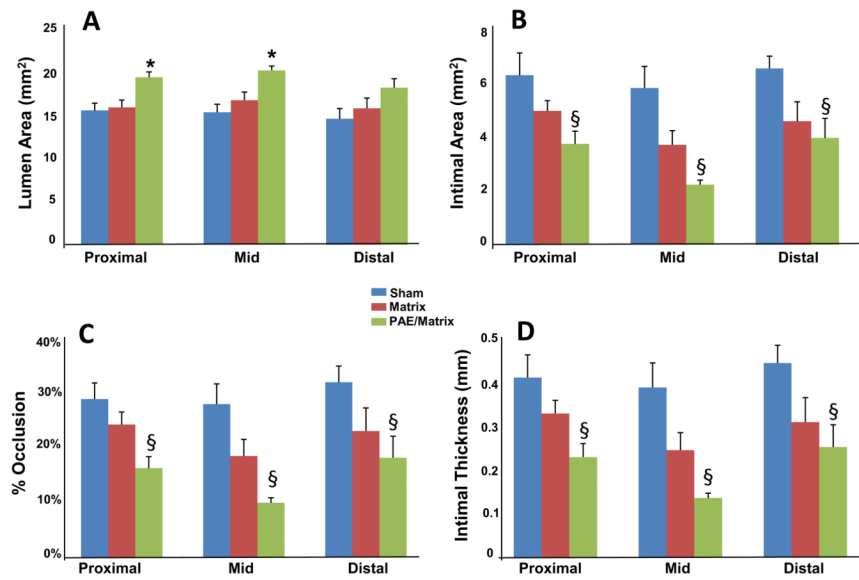


**Fig 4.**

Bar graphs of tissue plane analysis. (A) Lumen area,  $*P < .05$  compared with sham and matrix control groups; (B) intimal area; (C) % occlusion; and (D) intimal thickness,  $\$P < .05$  compared with sham control group. There was no statistical difference between the sham and matrix control groups when comparing the proximal, mid, or distal planes. *PAE*, Porcine aortic endothelial cells.

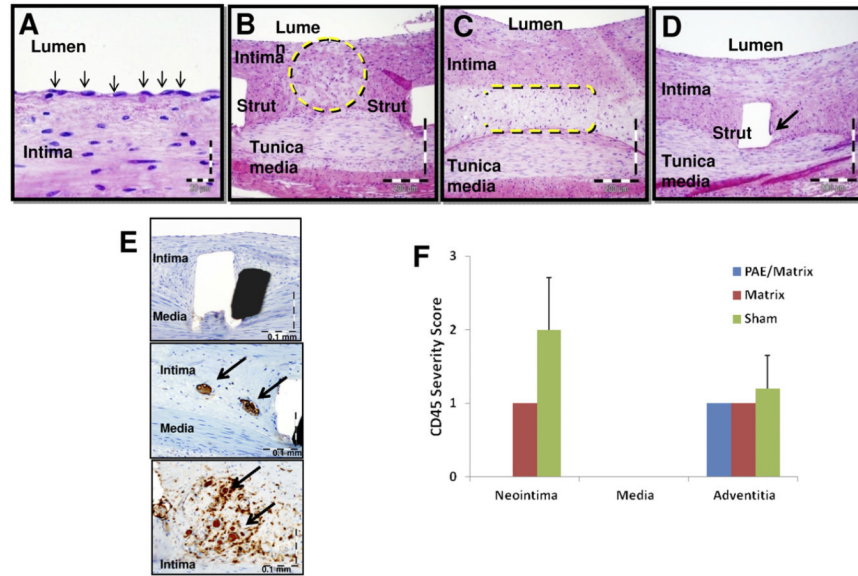


**Fig 5.** Representative photomicrographs of hematoxylin and eosin-stained arterial cross-sections depict (A) stent endothelialization (*arrows*), (B) reduced hypocellularity in porcine aortic endothelial cells (PAE)/matrix group (*dashed circle*) compared with (C) control matrix group (*dashed brackets*), (D) minimal inflammation associated with stent struts (*arrow*) in PAE/matrix group. E, Representative photomicrographs of CD45-stained arterial cross-sections depict no positive staining in the intima of PAE/matrix arteries (*top panel*) and moderate positive staining in the control matrix (*middle panel*) and sham (*bottom panel*) groups. *Arrows* point to positive CD45 staining. F, Bar graph demonstrates fewer CD45-positive leukocytes (severity score =  $0 \pm 0$ ) present in the intima of day 90 PAE/matrix animals compared with control matrix (severity score =  $1 \pm 0$ ) and sham (severity score =  $2 \pm 0.8$ ) groups.

**Table I**  
**Primer sets for real-time polymerase chain reaction**

<b>Genes</b>	<b>Functional pathways</b>	<b>Primers sequences (5'-3')</b>
Vascular adhesion molecule-1	Inflammation	CTGTTGAGATCTCCCCTGGA CGCTCAGAGGGCTGTCTATC
Intercellular adhesion molecule-1	Inflammation	TCAAGGGTTGGGGTCAGTAG GAAGTGGCCCTCCATAGACA
Tissue factor	Coagulation	ACCTCGGACAGCCAACAATTCAGA
	Thrombosis	ATCCCGGAGGCTTAGGAAAGTGTT
E-selectin	Inflammation	AGGTCCTTCTT CCT GCCAAGTGGTAA ATTGAGCGTCCATCCTTCAGG ACA
Interleukin-8	Inflammation	AGAAACCACCGGAAGGAACCATCT
	Smooth muscle cell activation	AGAGCTGCAGAAATCAGGAAGGCT
Hypoxanthine ribosyltransferase	Metabolism	AGATGGTCAAGGTCGCAAGC
	House-keeping	GGACTCCAGATGTTTCCAAACTCAAC

Table II

## Quantitative angiography of porcine-stented femoral arteries

Treatment	Artery (mm) <sup>a</sup>	B/A ratio <sup>b</sup>	Acutegain (mm) <sup>c</sup>	MLD (mm) <sup>d</sup>	Late loss (mm) <sup>e</sup>	% Stenosis <sup>f</sup>
Sham	3.65 ± 0.08	1.46 ± 0.09	0.91 ± 0.11	4.03 ± 0.16	0.72 ± 0.49	15.0 ± 4.0
Matrix	4.23 ± 0.27	1.21 ± 0.07	0.61 ± 0.55	4.01 ± 0.20	0.85 ± 0.40	17.0 ± 4.0
PAE/matrix	4.27 ± 0.16	1.21 ± 0.04	0.99 ± 0.35	4.72 ± 0.12 <sup>g</sup>	0.45 ± 0.29	10.0 ± 2.0

PAE, Porcine aortic endothelial cells

<sup>a</sup> Artery, preinjury.

<sup>b</sup> B/A, Balloon/artery.

<sup>c</sup> Acute gain (deploy – artery).

<sup>d</sup> MLD, Minimum lumen diameter measured on day 90.

<sup>e</sup> Late loss (deploy – MLD).

<sup>f</sup> % Stenosis = (ref vessel – MLD)/(ref vessel) × 100.

<sup>g</sup>  $P < .05$  compared with control arteries.

**Table III**  
**Histopathological characteristics of stented porcine femoral arteries**

Characteristics	Sham	Matrix	PAE/matrix
Number of arteries, n	6	5 <sup>a</sup>	6
Intima area (mm <sup>2</sup> )	6.2 ± 0.5	4.4 ± 0.5 <sup>b</sup>	3.3 ± 0.4 <sup>b</sup>
Neointimal thickness (mm)	0.40 ± 0.03	0.29 ± 0.04	0.20 ± 0.02 <sup>b</sup>
Lumen area (mm <sup>2</sup> )	16.1 ± 0.9	17.1 ± 1.0	20.43 ± 0.70 <sup>b</sup>
Lumen/artery ratio	0.65 ± 0.02	0.72 ± 0.03	0.77 ± 0.02 <sup>b</sup>
Stent diameter (mm) <sup>c</sup>	5.5 ± 0.13	5.4 ± 0.07	5.6 ± 0.04
% Occlusion <sup>d</sup>	28 ± 2.1	21 ± 2.8	14 ± 1.8 <sup>b</sup>

PAE, Porcine aortic endothelial cells.

<sup>a</sup>Right femoral artery of one control matrix animal removed from data analysis due to excessive procedural injury and subsequent intimal formation (complete occlusion).

<sup>b</sup> $P < .05$  compared with sham.

<sup>c</sup>Stent diameter ( $S_d$ ) =  $2 \times (S_a/\pi)$ .

<sup>d</sup>% Occlusion =  $(I/I + L) \times 100$ .

**Table IV**  
**Semiquantitative histomorphology<sup>19</sup>**

Characteristic	Sham	Matrix	PAE/matrix
Intimal fibrin	0.06 ± 0.04	0.0 ± 0.0	0.0 ± 0.0
Endothelialization <sup>a</sup>	4.0 ± 0.0	4.0 ± 0.0	4.0 ± 0.0
Adventitial fibrosis	1.0 ± 0.32	0.33 ± 0.27	0.72 ± 0.16
Neointimal hypocellularity <sup>b</sup>	1.33 ± 0.12	1.1 ± 0.22	0.44 ± 0.14 <sup>c</sup>
Medial smooth muscle cell necrosis	0.28 ± 0.13	0.0 ± 0.0	0.06 ± 0.06
Adventitial vascularization	0.0 ± 0.0	0.0 ± 0.0	0.0 ± 0.0
Inflammation <sup>d</sup>	0.61 ± 0.04	0.53 ± 0.09	0.60 ± 0.16
Injury score <sup>e</sup>	0.04 ± 0.04	0.0 ± 0.0	0.1 ± 0.04

PAE, Porcine aortic endothelial cells.

<sup>a</sup>Endothelialization was scored on a scale from 0 to 4 (0 = absent; 1 < 25%; 2 = 25-75%; 3 > 75%; 4 = 100%) and depended upon the extent of the circumference of the artery lumen showing coverage with endothelial cells.

<sup>b</sup>Characterized by areas of neointima with increased interstitial matrix within/around smooth muscle cells.

<sup>c</sup> $P < .05$  compared with control arteries.

<sup>d</sup>Sum of strut inflammation scores/No. of stent struts.

<sup>e</sup>The injury score depended on the part of the arterial wall perturbed by the stent. Injury was scored from 0 to 3 on a per-strut basis and the average was calculated per plane (0 = IEL intact; 1 = IEL disrupted; 2 = tunica media disrupted; 3 = tunica adventitia disrupted).